Biochimica et Biophysica Acta 1787 (2009) 86–96

Contents lists available at ScienceDirect

Biochimica et Biophysica Acta

journal homepage: www.elsevier.com/locate/bbabio

Purification, characterization and crystallization of menaquinol:fumarate oxidoreductase from the green filamentous photosynthetic bacterium *Chloroflexus aurantiacus*

Yueyong Xin [a], Yih-Kuang Lu [b], Raimund Fromme [b], Petra Fromme [b], Robert E. Blankenship [a,*]

[a] Departments of Biology and Chemistry, Washington University, Campus Box 1137, One Brooking Drive, St. Louis, MO 63130, USA
[b] Department of Chemistry and Biochemistry, Arizona State University, Tempe, AZ 85287, USA

ARTICLE INFO

Article history:
Received 29 April 2008
Received in revised form 20 November 2008
Accepted 21 November 2008
Available online 6 December 2008

Keywords:
Menaquinol:fumarate oxidoreductase
Purification
Characterization
Crystallization
Electron transfer chain
Chloroflexus aurantiacus

ABSTRACT

The integral membrane protein complex, menaquinol:fumarate oxidoreductase (mQFR) has been purified, identified and characterized from the thermophilic green filamentous anoxygenic photosynthetic bacterium *Chloroflexus aurantiacus*. The complex is composed of three subunits: a 74 kDa flavoprotein that contains a covalently bound flavin adenine dinucleotide, a 28 kDa iron-sulfur cluster-containing polypeptide, and a 27 kDa transmembrane polypeptide, which is also the binding site of two *b*-type hemes and two menaquinones. The purified complex has an apparent molecular mass of 260 kDa by blue-native PAGE, which is indicative of a native homodimeric form. The isolated complex is active in vitro in both fumarate reduction and succinate oxidation. It has been analyzed by visible absorption, redox titration, chemical analysis and EPR spectroscopy. In addition, phylogenetic analysis shows that the QFR of both *C. aurantiacus* and *Chlorobium tepidum* are most closely related to those found in the delta-proteobacteria. The purified enzyme was crystallized and X-ray diffraction data obtained up to 3.2 Å resolution.

1. Introduction

Quinol:fumarate oxidoreductase (QFR, EC 1.3.5.1) is a membrane-bound enzyme that catalyzes the reduction of fumarate to succinate and participates in the energy conservation mechanism of anaerobic organisms. It shows sequence similarity to succinate:quinone oxidoreductase (SQR) that catalyzes the reverse reaction of QFR and is involved in the citric acid cycle and respiratory electron transport [1–3]. The structures of *Wolinella succinogenes* QFR [4], *Escherichia coli* QFR [5], *E. coli* SQR [6] and mitochondrial SQR [7] have been solved by X-ray crystallography, demonstrating that the SQR/QFRs presumably evolved from a common primordial precursor and therefore possess a high degree of similarity with respect to their overall composition and cofactor requirement. However, QFRs form homodimeric complexes, whereas the SQRs form homotrimeric complexes. The family of SQR/QFR is classified into five types based on differences in the subunit composition and the number of the bound hemes [1,8]. Of these types, type B has a single polypeptide and 2 type B hemes in their integral membrane subunit (Cp), while the catalytic flavin adenine dinucleotide containing subunit (Fp) and iron-sulfur clusters containing subunit (Ip) are similar within the SQR/QFR family. The redox cofactors are separated by 9–17 Å from each other and are capable of electron transport. How the electrons flow between the substrate and the quinones through these cofactors is an intriguing question and been debated for a long time [1,2,8]. Very recently, this has been resolved for the most important controversial issues [9]. SQR and/or QFR enzymes have also been extensively investigated in different species such as *Acidianus ambivalens*, *Rhodothermus marinus*, *Desulfovibrio gigas*, *Corynebacterium glutamicum*, *Geobacter sulfurreducens*, *Helicobacter pylori* and *Campylobacter jejuni* [10–15]. However, so far the complexes studied by X-ray crystallography are all from non-photosynthetic species.

Chloroflexus aurantiacus is a green Filamentous Anoxygenic Phototrophic bacterium (FAP) [16]. Based on the bacterial 16 S rRNA tree of life [17], *Chloroflexus* is not closely related to any other groups of photosynthetic bacteria. In fact, it forms a very deep division within the eubacterial line of descent, forming the only phototroph-containing branch occurring prior to the nearly simultaneous radiation of all the other bacterial phyla, which has significance in the evolution of photosynthesis [18]. It can grow both as an anaerobic phototroph in the light and an aerobic chemotroph in the dark. No significant differences in cell shape or dimensions between aerobically and phototrophically grown cells were observed [19]. Also, there is no

Abbreviations: mQFR, menaquinol fumarate oxidoreductase; SQR, succinate quinone oxidoreductase; FAD, flavin adenine dinucleotide; Em, redox midpoint potential; DDM, dodecyl maltoside; PMS, phenazine methosulfate; DCPIP, 2,6-dichloro-phenolindophenol; HQNO, heptyl-4-hydroxyquinoline N-oxide; Fp, FAD-containing subunit; Ip, Iron-sulfur-cluster containing subunit; Cp, Cytochrome containing membrane anchor subunit

* Corresponding author. Tel.: +1 314 935 7971; fax: +1 314 935 4432.
E-mail address: blankenship@wustl.edu (R.E. Blankenship).

0005-2728/$ – see front matter © 2008 Elsevier B.V. All rights reserved.
doi:10.1016/j.bbabio.2008.11.010

differentiation of the cytoplasmic membrane during the photosynthetic apparatus formation, which suggests that in both photosynthesis and respiration electrons will traverse a membrane-associated electron transport chain, involving menaquinone, the only quinone present in *Chloroflexus* [20]. This electron transfer chain has to involve transmembrane complexes, of which several complexes have so far been identified in *Chloroflexus* at the protein and gene level [21]. Unlike these complexes, QFR has not been purified and characterized in most photosynthetic species. However, *b*-type cytochromes were found to be present in the membrane [22,23]. Recently, two multisubunit complexes containing cytochrome *c* have been isolated from *Chloroflexus* membranes and one of them is proposed to fulfill the proton translocation function that is usually carried out by the cytochrome bc_1 complex [23,24].

In this paper, the purification and characterization of the mQFR complex from *Chloroflexus* is reported. The purified enzyme is homogeneous and has been crystallized and diffraction data obtained to 3.2 Å resolution. Finally, the possible functions of the QFR are discussed, considering related experimental and structural data.

2. Materials and methods

2.1. Bacterial strain and growth

Anaerobic cells of *C. aurantiacus J-10-fl* were grown in medium DG either in 1000 mL culture bottles in an incubator or in a 14-liter fermentor stirred at 200 rpm at 3000 lx light intensity as described previously [25]. Cells were harvested in exponential growth phase by centrifugation at 12,000 g for 15 min and washed twice with 50 mM Tris–HCl buffer, pH 8.0 (buffer A) and stored at −80 °C.

2.2. Purification of mQFR complex

Harvested cells were broken by passage through a French Pressure Cell three times at 20,000 psi in the presence of DNase and $MgCl_2$. Unbroken debris were removed by centrifugation at 12,000 ×*g* for 10 min. The supernatant liquid was then ultracentrifuged at 200,000 ×*g* for 2 h. The pellets were used as whole membranes, which were resuspended in buffer A and adjusted to OD_{866}=10. The detergent, reduced Triton X-100, was added dropwise to final a concentration of 4% (w/v), and the solution was incubated at room temperature for 1 h with stirring. After centrifugation at 200,000 ×*g* for 2 h, the supernatant was collected and loaded onto a Q Sepharose Fast Flow 26/20 column. The column was washed extensively with buffer A containing 0.25% reduced Triton X-100 until the green color due to solubilized free pigment BChl *c* was removed, then the crude mQFR was eluted with a linear gradient of NaCl from 0.1 M to 0.5 M in 20 times of column volume. Appropriate fractions were collected and diluted with buffer A containing 0.05% dodecyl maltoside (DDM). A second ion exchange chromatography (IEC) on Q Sepharose High Performance 5 mL column was carried out. Further purification by gel filtration on S-300 26/70 gel filtration column in 20 mM Tris–HCl, pH 8.0, 0.02% DDM, 100 mM NaCl, and a final purification using a Mono Q1 column with a Bio-Rad Duo-Flow chromatography system. Finally, the preparation was concentrated to A_{415}=40 using a Centricon–100 centrifugal filter.

2.3. Enzyme activity measurements

Succinate: acceptor oxidoreductase activity was measured with PMS (0.5 mg/mL) and DCPIP (20 μg/mL) as electron acceptors. In this assay, electrons are transferred from succinate (20 mM) via the isolated protein complex (0.5 μg) to PMS then to the final electron acceptor, DCPIP. Reduction of DCPIP was measured spectrophotometrically by the decrease in the absorbance at 600 nm (ε=20.7 mM^{-1} cm^{-1}). The QFR activity assays were performed in an anaerobic cuvette at the following final concentrations of 200 μM 2-methyl-1,4-napthoquinone reduced by $NaBH_4$, 20 mM potassium fumarate, and 0.2 μg mQFR complex.

2.4. Chemical analysis methods

Protein concentration was determined using the bicinchoninic acid procedures (Pierce) with bovine serum albumin as standard. SDS-PAGE and Blue-Native Gel electrophoresis were performed as described previously [26,27]. FAD content was determined as acid-nonextractable flavin essentially as described previously [28]. Acid-labile sulfur content was determined as described previously [29]. Total iron content was measured by the inductively coupled plasma mass spectrometry. Heme content was determined from the pyridine hemochromogen difference spectrum using the extinction coefficients 23.98 mM^{-1} cm^{-1} (558 nm minus 540 nm) or 29 mM^{-1} cm^{-1} (558 nm minus 570 nm) [30]. Quinone content was determined as described previously [31].

2.5. In-gel protein digestion

Stained bands of the subunits were excised, in-gel digested with trypsin, and extracted from the gel as described previously [32] with the following modifications. The excised protein band was destained and washed with 100 mM NH_4HCO_3. Proteins were then reduced by 20 mM DTT, 100 mM NH_4HCO_3 for 1 h at 55 °C. Cysteines were further alkylated by 55 mM iodoacetamide in 100 mM NH_4HCO_3 for 45 min at room temperature. Trypsin (Promega Trypsin Gold, TPCK treated) in 50 mM NH_4HCO_3 was added to the gel pieces in an Eppendorf tube and the enzymatic reaction was carried out overnight at 37 °C. Peptides were extracted twice in 50 μL of 5% formic acid, 50% acetonitrile for 20 min. Extracts were collected, dried completely in a speed-vac, redissolved in 50% acetonitrile containing 0.1% trifluoroacetic acid, and desalted by ZipTipC18 (Millipore, Billerica, MA).

2.6. MALDI-TOF analysis and database search

MALDI-TOF analyses were used to determine both intact protein molecular weights and protein identities by peptide mass fingerprinting. Analysis was performed using Voyager DE STR MALDI-TOF mass spectrometer (Applied Biosystems, USA). 1 μL of the sample mixed with 1 μL of freshly prepared matrix solution was spotted on a stainless steel sample plate. Sinapinic acid was used for intact protein analysis and α-cyano-4-hydroxycinnamic acid for peptide mass fingerprinting. Each mass spectrum was the average of at least 100 laser shots and calibrated by Data Explorer software (Applied Biosystems, USA). Calibration was performed using equine cytochrome *c* (12,270), bovine serum albumin (66,200) for intact protein and angiotensin1 (1296.685), ACTH clip1-17 (2093.087), ACTH clip 18-39 (2465.199), ACTH clip7-38 (3657.929), and bovine insulin (5730.609) for peptide mass fingerprinting. Intact protein mass spectra were acquired using instrument parameters in order to achieve an expanded spectral range: *m*/*z* 20,000 to 80,000. Peptide masses were acquired with a range of ca. *m*/*z* 600 to 8,000.

Peptide mass values searches were performed against the National Center for Biotechnology Information (NCBI) sequence (NCBInr) database using MASCOT Peptide Mass Fingerprint database search software (www.matrixscience.com). The alkylation of cysteine was included as a possible modification. One missed tryptic cleavage was considered, and the mass tolerance for the monoisotopic peptide masses was set to ±0.15 Da.

2.7. Phylogenetic analysis

Phylogenetic analysis was performed using the amino acid sequences of the subunit of QFR or SQR from various species. Protein

Table 1
Purification protocol of mQFR complex from *C. aurantiacus*

Isolation step	Volume (mL)	Protein (mg)	Cyt *b* (nmol)	Yield (%)
Whole membrane	200	4000	1730	100
Triton extract	300	1789	850	49
1st IEC	150	667	326	19
2nd IEC	45	340	290	16
S-300 Gel Filtration	15	200	232	13
Mono Q IEC	5	180	203	11

sequences were retrieved from public databases using the NCBI protein query tools. Alignment and phylogenetic tree construction were carried out by MEGA software, version 3.1. The default parameters were used. The phylogenetic trees shown were derived from analyses of each subunit sequences with highly conserved topology. The neighbor-joining method was performed for the construction of the phylogenetic trees.

2.8. Redox potential titration

Redox titrations were done as described previously [33] and conducted by using a reaction mixture containing preparations (5 mg protein/mL) suspended in 20 mM Tris buffer (pH 7.0) in anaerobic conditions. The following redox mediators were also present: 20 μM ferricyanide; 50 μM hydroquinone; 50 μM diaminodurene; 50 μM 1,2-naphthoquinone; 100 μM duroquinone; 25 μM PMS; 25 μM phenazine ethosulfate and 25 μM anthroquinone disulfonate. The titration was conducted at 25 °C. Desired ambient potential values were adjusted by additions of buffered solutions of sodium dithionite or potassium ferricyanide. All potentials stated are relative to the standard hydrogen electrode. Reduction of Cyt *b* was recorded as the difference in absorbance between the α-band maximum at 558 nm and the isosbestic point at 570 nm. The redox midpoint values were calculated from data by fitting with the Nernst equation using Origin 7.5.

2.9. EPR spectroscopy

For EPR analysis of purified enzyme at different redox potentials, aliquots were anaerobically transferred from the titration vessel with a gas-tight long needle syringe to calibrated quartz EPR tubes, frozen, and stored at 77 K for later analysis. The spectra were recorded with a Bruker ER 200D-SRC X-band spectrometer equipped with an Oxford ESR-9 liquid helium cooling system. EPR instrument settings: frequency, 9.21 GHz; microwave power, 10 mW; field modulation,

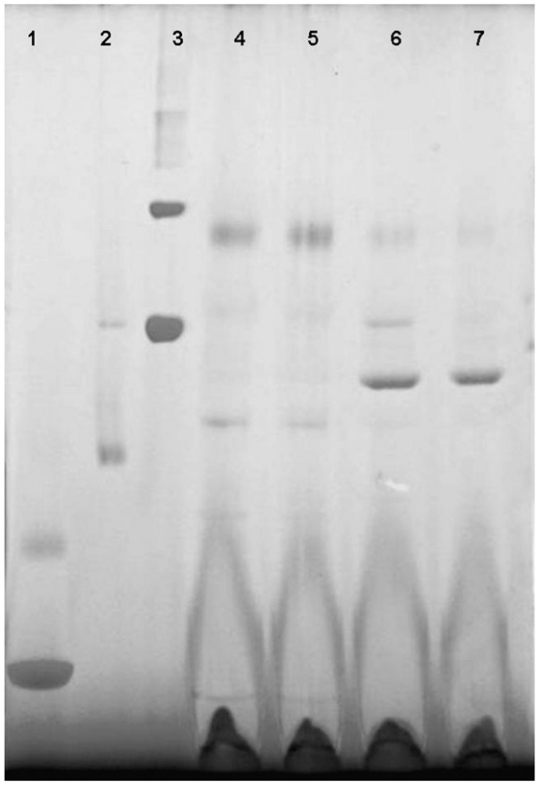

Fig. 2. Blue-Native PAGE analysis of mQFR complex purified from *Chloroflexus aurantiacus*. Lane 1, standard protein 1: BSA (monomer 66 kDa, dimer 132 kDa); lane 2, standard protein 2: catalase (monomer 230 kDa, dimer 460 kDa); lane 3, standard protein 3: ferritin (monomer 440 kDa, dimer 880 kDa); lane 4 and 5, ATP synthase (550 kDa); lane 6, mQFR complex after gel filtration; lane7, purified mQFR complex (260 kDa).

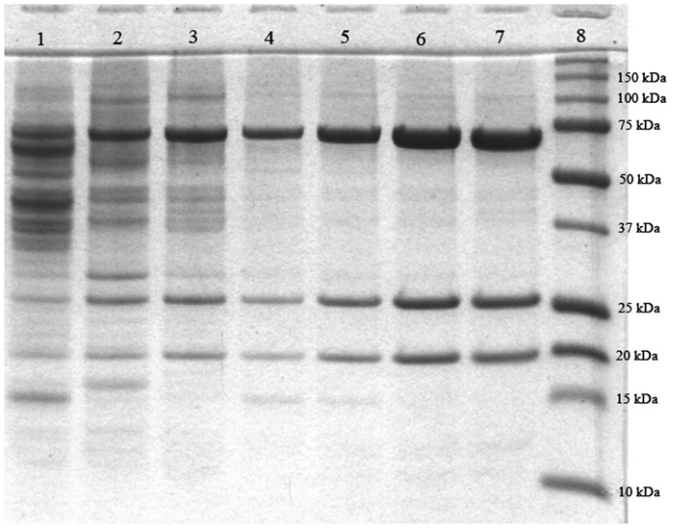

Fig. 1. SDS-PAGE analysis of polypeptide composition of mQFR samples from different purification steps by using a 12.5%T, 3%C gel system. Lane 1, purified cytoplasmic membrane; lane 2, proteins extracted with detergent; lane3, peak fraction from first ion exchange chromatography; lane 4, peak fraction from second ion exchange chromatography; lane 5, peak fraction from S-300 gel fraction column; lane 6 and lane 7, peak fraction from Mono Q column; lane 8, precision plus protein standards from Bio-Bad. Total protein concentration in each lane is about 35 μg.

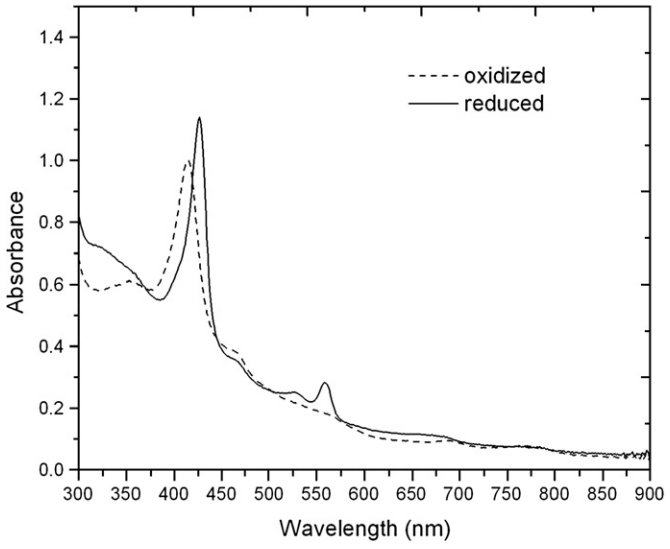

Fig. 3. UV–visible light absorption spectra of the mQFR complex purified from *Chloroflexus aurantiacus* at room temperature. Absolute spectra of the air-oxidized (dashed lines) and dithionite-reduced forms (solid lines).

Table 2
Chemical composition analysis of the purified *C. aurantiacus* mQFR complex

Component	Content (nmol/mg of protein)	Stoichiometry relative to FAD
FAD	2.9±0.1	1
Heme b	6.1±0.2	2
[Sulfur]	33±0.1	10
Iron	32 ± 0.2	11
Quinone	4.8±0.1	1.6

10 G; gain, 50; temperature, 20 K. EPR spectra analysis were performed by WINEPR software.

2.10. Crystallization

The hanging drop vapor diffusion method was used with crystallization plates from Hampton Research, California. The oxidized mQFR was crystallized in the presence of 0.02% DDM, 0.1 M NaCl, 0.2% decyl maltoside, 2.2% benzamidine, 2 mM fumarate at protein concentration of 10 mg/mL. The reservoir solution was 0.1 M citrate, pH 5.6 containing 0.15 M NaCl, 10–12% PEG-6000.

3. Results

3.1. Purification and characterization

The mQFR complex of *C. aurantiacus* was isolated from the cytoplasmic membrane by extraction with the detergent, reduced Triton X-100, and purification in another detergent, DDM, in four chromatography steps. A purification protocol for a typical preparation is given in Table 1. The total recovery was about 11%. The apparent succinate dehydrogenase activity of the enzyme increased during the purification process. The purified enzyme catalyzes fumarate reduction as well as succinate oxidation with commensurate activities. The specific activity of purified enzyme is 18–20 μmol substrate per min per mg protein. It is not restricted to menaquinone, the in vivo quinone in this species. In addition, the reaction of fumarate reductase is insensitive to the enzyme inhibitor HQNO. This is consistent with the results of *Bacillus subtilis* SQR and *W. succinogenes* QFR [28,34].

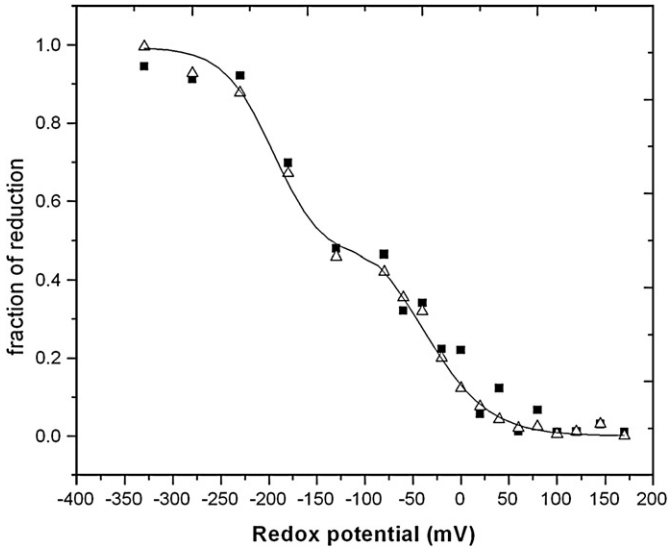

Fig. 4. Redox potential titration analysis of mQFR complex purified from *Chloroflexus aurantiacus*. The plots are combined results from four titrations of both reduction (solid square) and oxidation (open triangle). The solid line is the fitting curves according to Nernst equation (n=1), assuming that half of absorbance is derived from high potential heme (Em=−40 mV) and another half from low potential heme (Em = −190 mV).

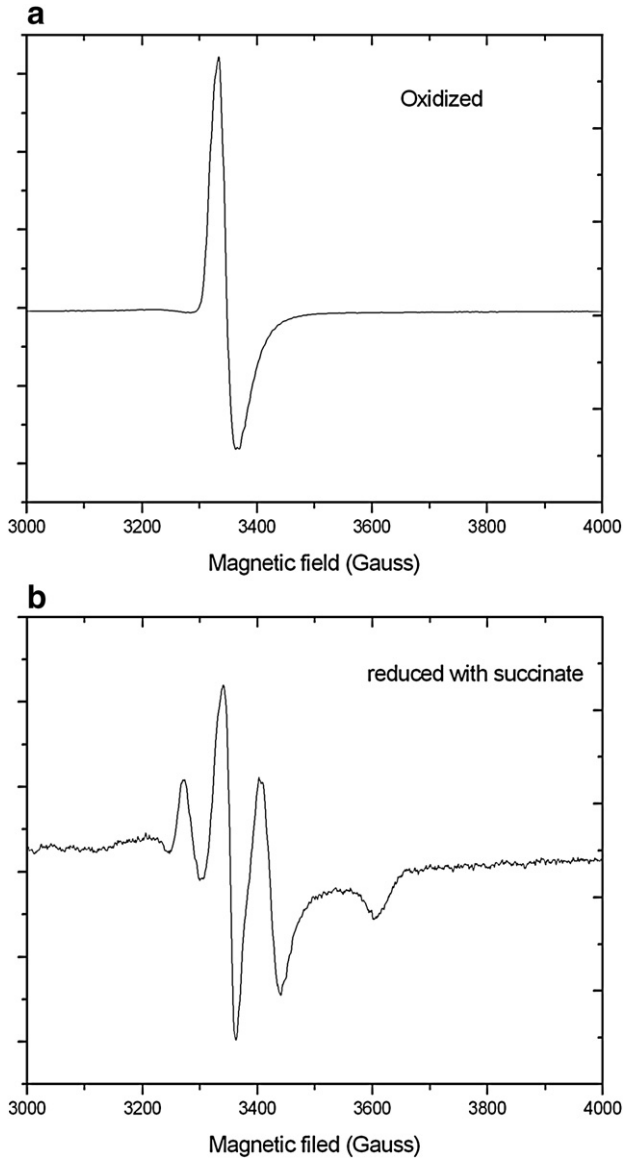

Fig. 5. EPR Spectra of mQFR complex purified from *Chloroflexus aurantiacus* showing signals from oxidized state (upper) and succinate-reduced state (lower).

However, the in vitro conditions poorly reflect the different substrate availabilities in the cell and the data are not sufficient to determine the real reaction direction, or if the complex is bidirectional [14].

The polypeptide compositions of samples from the different purification steps are shown in Fig. 1. Judging from the SDS-PAGE gel, stained for protein with Coomassie brilliant blue G-250, the isolated mQFR complex was at least 95% pure. The stoichiometry of Fp: Ip: Cp subunits has been determined as 1: 1: 1 by analysis of the

Table 3
The result of mass finger printing for the identification of QFR subunits in *Chloroflexus aurantiacus* genome

Subunit	Access number[a]	Number of amino acids[a]	M_r/kDa[a]	pI[a]	Fragments identified[b]	MASCOT score[b]	Percent sequence coverage[b]
Fp	gi76261585	657	73.2	8.6	32	118	56%
Ip	gi76261584	260	28.1	5.4	27	84	58%
Cp	gi76261586	239	27.1	9.7	10	70	31%

[a] Provided by National Center for Biotechnology Information (NCBI) database.
[b] Provided by MASCOT Peptide Mass Fingerprint database search software (www.matrixscience.com).

staining pattern. Thus, the molecular weight of the mQFR complex would be about 130 kDa if it is a monomer. However, the result of blue-native gel electrophoresis (Fig. 2) reveals that the molecular weight of the isolated complex is about 260 kDa. This suggests that the functional complex probably is a dimer, which is consistent with the homodimers proven experimentally for the mQFRs from *W. succinogenes*, *H. pylori*, and *C. jejuni* [15].

UV–visible absorption spectra at room temperature of isolated mQFR complex are shown in Fig. 3. The oxidized enzyme shows protein absorption at 275 nm and a cytochrome Soret band at 415 nm. Addition of succinate results in partial reduction of the cytochrome, gives a spectrum with absorption maxima at 558 and 528 nm (α- and β-bands), and causes a shift in the Soret peak to 424 nm. The UV–Vis absorption spectra indicate that Cyt *b* is reduced to about 50% with succinate compared to that with dithionite.

The chemical composition of the purified QFR complex is presented in Table 2. The stoichiometric ratio between covalently bound FAD and the iron-sulfur cluster, representing the Fp and Ip subunits respectively, was found to be 1:1. Protoheme IX was present in about 2:1 stoichiometry to covalently bound FAD, demonstrating the presence of two hemes per complex. About 11 iron atoms per complex were found, which is expected if the enzyme contains one [2Fe–2S] cluster, one [3Fe–4S] cluster, one [4Fe–4S] cluster and two type *b* hemes as is typically found in other examples of this same type of enzyme. From these combined results, we conclude that Cyt *b*558 is a diheme cytochrome. In the redox titration shown in Fig. 4, half of the heme *b* in the enzyme exhibited a midpoint potential of −40 mV, whereas the other half was at −190 mV, relative to the standard hydrogen electrode. The simplest interpretation of these results is that the proximal heme group is the high-potential and the distal one low-potential. Each heme component contributes approximately 50% to the total absorption at 558 nm of the fully reduced cytochrome. The assignment of the high-potential heme to the proximal position in the structure is consistent with that for *W. succinogenes* mQFR [35].

As shown in Fig. 5, EPR spectroscopy indicates the purified mQFR complex has two iron-sulfur centers of the ferredoxin type that are paramagnetic in the reduced state (2Fe–2S and 4Fe–4S) and one iron-sulfur center of the high potential type that is paramagnetic in the oxidized state (3Fe–4S). Centers 2Fe–2S and 4Fe–4S exhibit a large difference in their redox midpoint potential: center 2Fe–2S is reducible with succinate, whereas the latter one can only be reduced by very low potential reductant such as dithionite.

3.2. Identification by MALDI-TOF MS and phylogenetic analysis

Each subunit of the mQFR complex observed in SDS-PAGE was excised, washed, and digested with trypsin. Resulting peptides were analyzed using peptide fingerprinting mass spectroscopy as described previously [24,32]. The obtained peptide mass spectra were used for a search by the MASCOT (Matrix Science) software for protein identification. A search was conducted against the *C. aurantiacus* genome and the NCBI protein database. The *C. aurantiacus* mQFR was conclusively identified and all of the searching results are summarized in Table 3. Both the MASCOT score and the percent sequence coverage indicate reliable correspondence with respect to each sequence of mQFR subunits. Each identified sequence of mQFR subunits was then used as queries in BLAST searches against the *C. aurantiacus* genome. It was further confirmed that the *C. aurantiacus* genome sequence includes a putative operon encoding the mQFR. This operon encodes three subcomponents, which are the flavoprotein, iron-sulfur-binding protein, and cytochrome *b*. They are designated as frdA, frdB, and frdC, respectively (GeneBank accession No. EAO57712, EAO057711, and EAO057713).

Molecular weight of each intact subunit of the purified mQFR was determined by MALDI-TOF mass spectrometry (Fig. 6). The spectrum clearly showed five predominant MALDI-TOF peaks at *m*/*z* 74,018, 37,008, 28,064, 28,184, and 27,176 Da. No further peaks were detected beyond *m*/*z* 80,000 Da in the spectral analysis. We calculated the theoretical masses of 73,234, 28,064 and 27,097 Da with respect to the deduced amino acid sequences of flavoprotein, iron-sulfur protein, and cytochrome subunit. Here, we also note that the apparent cytochrome *b* mass of *C. aurantiacus* mQFR by SDS-PAGE mobility is slightly lower than that calculated from the amino acid sequence.

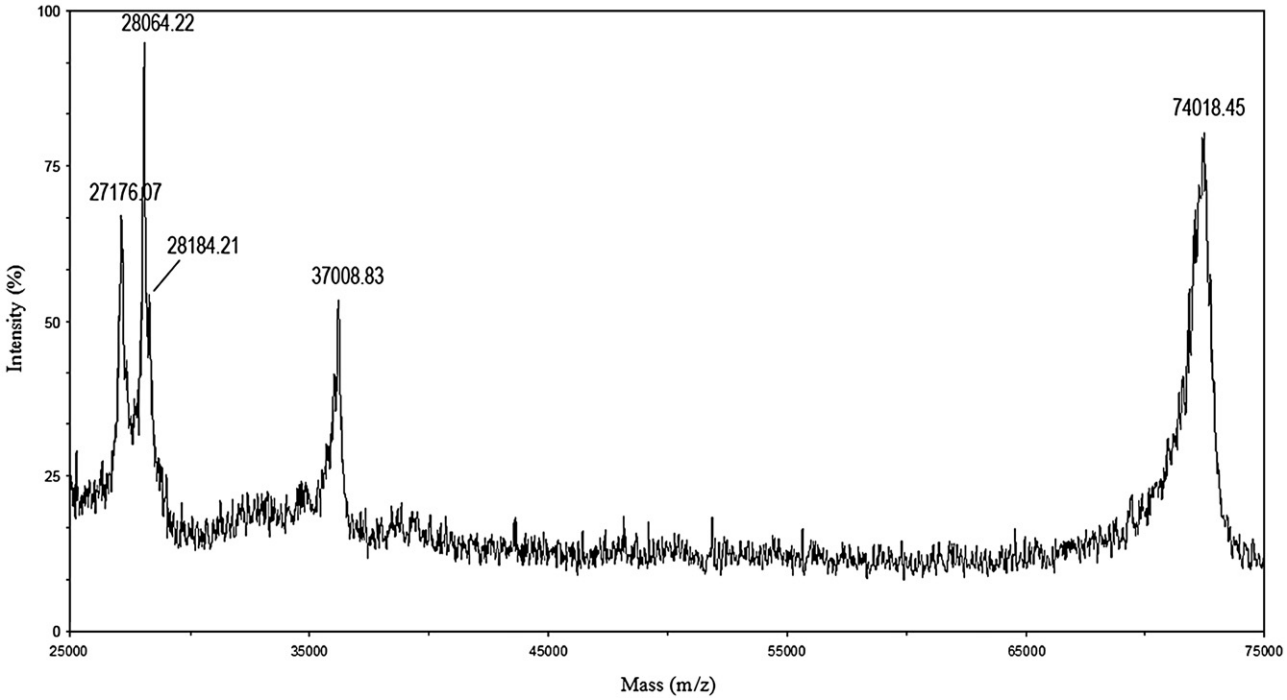

Fig. 6. MALDI-TOF mass spectrometry of mQFR whole protein from *Chloroflexus aurantiacus*. The peak at 74,018.45 Da is from Fp subunit, the peak at 37,008.83 Da is from doubly charged Fp subunit, the peaks at 28,184.21 Da and 28,064.22 Da are from Ip subunit, and the peak at 27,176.07 Da is from the Cp subunit.

For the largest subunit of *C. aurantiacus* mQFR, a difference of 783 Da is indicative of a covalently bound FAD^{+} cofactor in the flavoprotein. Notably, the peak at *m*/*z* 37,008 is for $(M+2H)^{2+}$of the Fp subunit. On the other hand, we have identified the peaks at 28,064 and 27,097 Da as representative of the Ip subunit and the Cp subunit without their prosthetic groups. The failure to identify both iron-sulfur cluster and heme results from the likely dissociation of these non-covalently bound cofactors in a denaturing condition when the

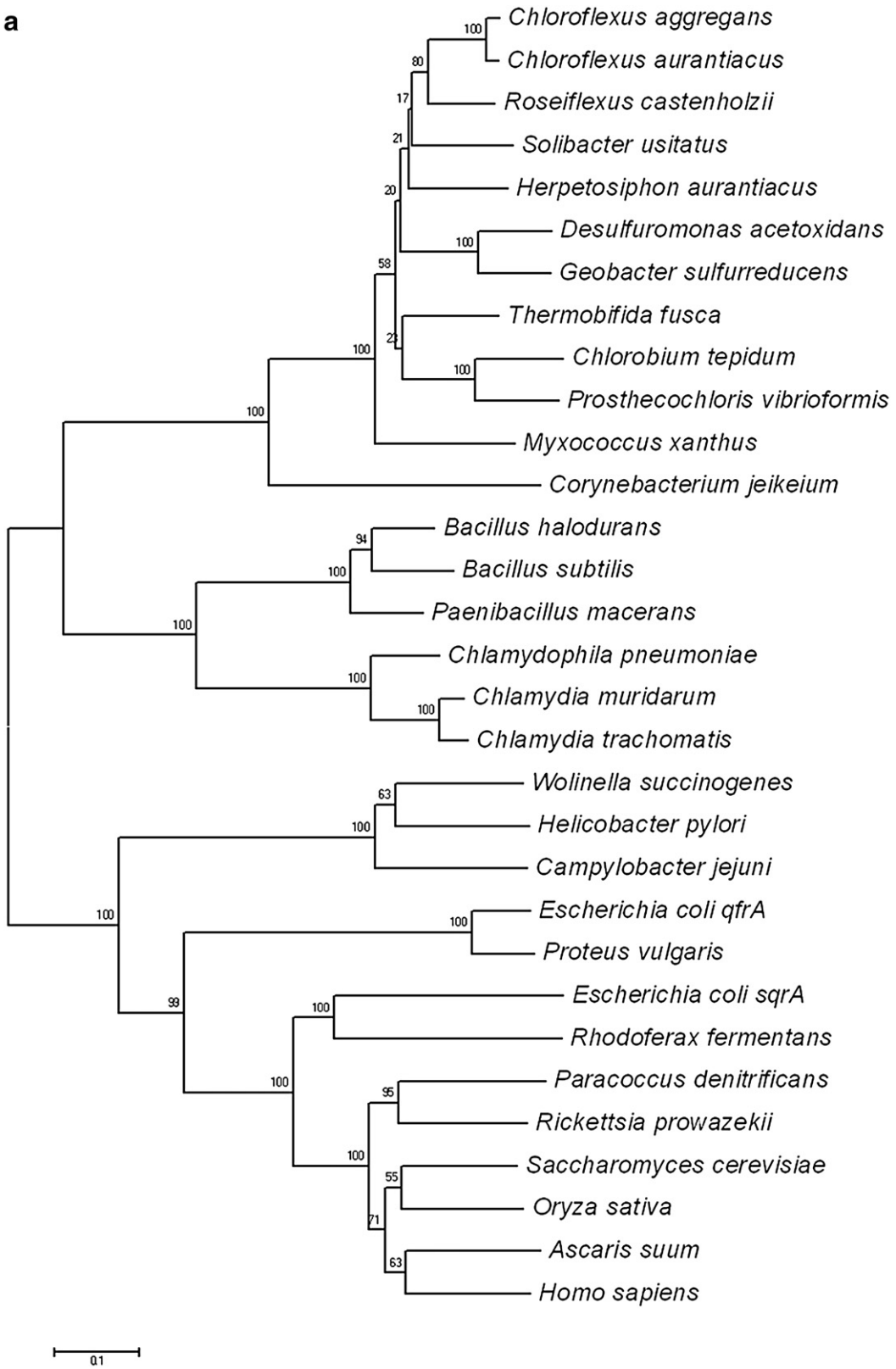

Fig. 7. Phylogenetic analysis of three subunits of mQFR complex. (A), FAD-containing subunit (Fp); (B) Iron-sulfur-cluster containing protein (Ip); (C) Cytochrome containing subunit (Cp).

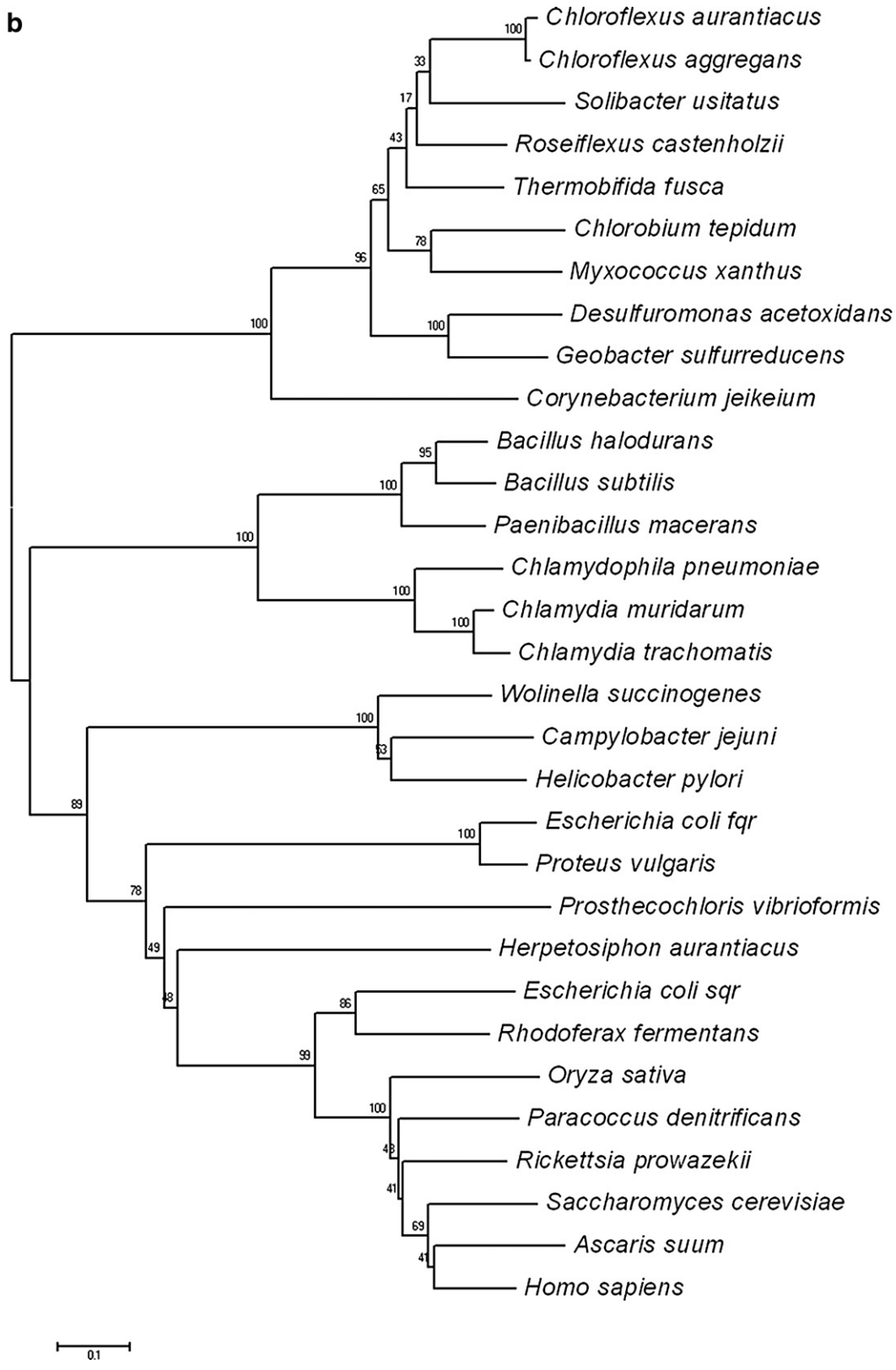

Fig. 7 (*continued*).

complex was dissolved in 50% acetonitrile/ 0.1% TFA. Nevertheless, the identified 120 Da difference of a minor peak at *m*/*z* 28,184 from 28,064 Da of the Ip subunit indicates the remaining residue of the non-covalently iron-sulfur clusters. Finally, with respect to the theoretical mass of 27,097 Da of the Cp subunit, the 79 Da difference as a phosphate modification was identified in the peak at *m*/*z* 27,176 Da. This modification might relate to the signal transduction for the regulation of metabolic function.

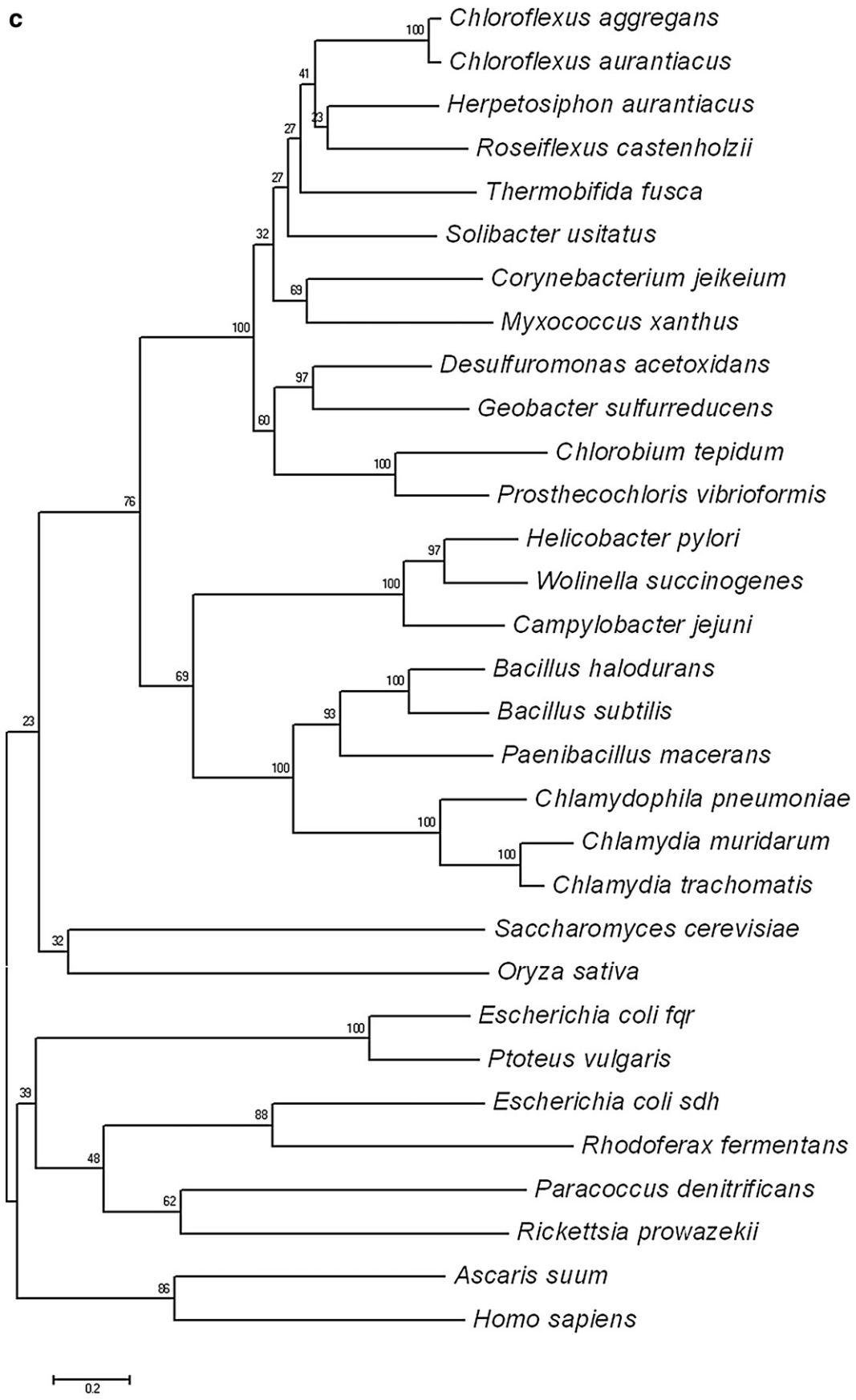

Fig. 7 (*continued*).

Because two core subunits, Fp and Ip, forming the hydrophilic domains are required for the catalytic function, it is hypothesized that a co-evolution of both components has occurred in both bacteria and eukaryotic mitochondria [8]. Thus, it prompted us to analyze the possible evolutionary origin of *C. aurantiacus* mQFR with respect to the possible origin of the cytochrome *b* containing subunit (Cp). The aligned sequences were analyzed (Supplemental Fig. S1) and used to construct a phylogenetic tree with respect to Fp, Ip, and Cp subunits, respectively (Fig. 7). Prokaryotic and eukaryotic QFR/SQR branched out into four groups (A–D) with high bootstrap values as observed in both Fp and Ip subunits. Nonetheless, we found that two species (*Herpetosiphon aurantiacus* and *Prosthecochloris vibrioformis*) have more variation in the amino acid sequence of the Ip subunit and thus belong to group D instead of group A. This observation is consistent with previous investigations [36]. On the contrary, the Cp subunit shows poor sequence similarities due to the various compositions of SQR/QFR. The divergence of the Cp subunit might be evolutionarily independent from the other two subunits [37]. The SQR/QFR family is classified into A–E types based on the differences in subunit composition and the number of bound hemes [1,8,38]. In the phylogenetic tree of the cytochrome subunit, both *Chloroflexaceae* (such as *C. aurantiacus*, *Roseiflexus castenholtzii* and *H. aurantiacus*) and *Chlorobiaceae* (such as *C. tepdium* and *Prosthecochloris vibriofomris*) families are closely related to the subgroup A, which also includes delta-proteobacteria. It seems that QFR/SQR of both *Chloroflexcease* and *Chlorobiaceae* families may share a common ancestor but have evolved independently.

3.3. Crystallization and X-ray diffraction

Purified mQFR complex appeared to be a homogeneous and monodisperse preparation; only one blue band was detected in Blue Native PAGE (Fig. 2) and only one elution peak was obtained from analytical gel filtration. Resolution by second dimension Tricine-SDS-PAGE confirmed that almost no impurities were present. We used the hanging drop vapor diffusion method for crystallization. For screening, we took the MembFac and Grid Screen kits from Hampton Research, California and after optimization of the preliminary conditions we obtained the single crystal that diffracts X-ray up to 3.2 Å (Supplemental Fig. S2). The shape and space group of our mQFR crystal are dissimilar to the crystals whose structure been solved by the same technique. The determination of the structure is in progress.

4. Discussion

4.1. Purification and identification

The cellular location of the photosynthetic apparatus in *C. aurantiacus* suggests that the development of the photosynthetic apparatus upon change to anaerobic light conditions may occur in the absence of membrane proliferation and differentiation of the cytoplasmic membrane [22]. This provides a simple system in which the regulation of electron flow between respiratory and photosynthetic electron transport chains can be studied. In the process of finding these common components of the two systems, we detected and isolated the mQFR complex and another complex, neither of which was previously known to be a component of photosynthetic membranes [24]. The *Chloroflexus* mQFR is functionally active in both anaerobic phototrophic and aerobic heterotrophic conditions.

The *C. aurantiacus* mQFR complex is a new member of type B of the SQR/QFR superfamily from a photosynthetic bacterium. This finding is very interesting since its detailed functional and structural studies would help us to better understand the electron transfer pathway and the hypothesis of co-evolution of both flavoprotein and the iron-sulfur protein. Since these two subunits of SQR/QFR from all species seem to have a common composition and function, it is believed that they have evolved together. SQR/QFRs from all species also seem to have a common origin, and was presumably present in the last common ancestor [8]. As shown in Fig. 7A, B, a similar phylogenetic pattern can be derived for subunits Fp and Ip. The proteins encoded by the frdA and frdB homologues showed 27 to 66% sequence identity for the Fp subunit, and 22 to 61% identity for the Ip subunit. Additionally, the sequence alignments (Supplemental Fig. S1) also indicate that the signal peptide at those eukaryotic sdhA/frdA and sdhB/frdB for the translocation to the mitochondria does not appear among the prokaryotic ones. This was proved experimentally that prokaryotic SQR/QFR components are assembled in the cytoplasm before being inserted into the membrane [39]. In the *frdA/sdhA* sequences alignment, the FAD-binding histidines, the six regions for AMP binding, and the active site histidine and arginine were found strictly conserved (Supplemental Fig. S1). In the *frdB/sdhB* sequence alignment, the highly conserved regions are three cysteine-rich clusters. It is noted that the cysteine residues in the first region are altered to serine in *H. aurantiacus* and an additional cysteine appears in the second and third regions in both *H. aurantiacus* and *P. vibrioformis*. As these two species belong to the *Choroflexus* and *Chlorobium* families, respectively, these significant variations may have an evolutionary meaning reflecting their particular metabolism. The similar replacement of cysteine by serine and/or aspartic acid has been observed in other species such as yeast, *E. coli* and *R. fermentans* [36].

Inspection of the sequence alignment for the membrane anchor corroborated that *C. aurantiacus* mQFR belongs to type B of QFR/SQRs superfamily. This is consistent with our other biochemical evidence. The Cp of *Chloroflexus* mQFR is predicted to form five membrane-spanning regions by hydropathy plot, similar to the corresponding proteins throughout the group. The axial heme ligand histidines identified throughout all of the aligned sequences are conserved in the corresponding regions, suggesting a similar structure and topology with the closely related delta-proteobacteria such as *Corynebacteria* and *Geobacteria*. The low amino acid sequence identity of the membrane anchor subunits, in contrast to the flavin and iron-sulfur ones, may be related to the fact that these subunits are subjected to a less intense evolutionary pressure. In fact, the maintenance of the secondary structure elements required for transmembrane attachment may be achieved by a quite diverse combination of amino acids. The role of the two heme groups in the diheme QFR/SQRs is to mediate efficient electron transfer across the cytoplasmic membrane and has recently been unambiguously demonstrated for *W. succinogenes* QFR [9]. The same general functional and structural arrangement of heme is known, or is anticipated, in a number of transmembrane diheme proteins with diverse biological function, e.g. iron reductase, dissimilatory nitrate reductase, and bacterial hydrogenase [40].

4.2. Physiological function of mQFR

The physiological roles of the newly isolated mQFR complex in the electron transport chain remain to be elucidated. The unique position of the similar complex as a member of both the citric acid cycle and the respiratory chain implies that it may have a key regulatory role when the bacterium is grown in aerobic conditions. Although the bacterium can grow anaerobically photosynthetically, it nonetheless contains a membrane-bound QFR, which was found in this study to have properties closely resembling those of the different type of SQR/QFR. The measured redox potentials of two hemes of the enzyme are similar to that of *W. succinogenes* QFR. When *Chloroflexus* cells live under strictly anaerobic conditions, the enzyme probably possesses a QFR instead of SQR activity as the quinone pool in the membrane should be mostly reduced by the photosynthetic reaction center. Also, although in general the QFRs have reduction potentials slightly lower than those of the SQRs, there is a considerable overlap of the potentials reported for both types of enzymes; this may explain why the enzymes are bi-

directional in the in vitro analysis as observed in other species [14]. The mQFR complex of *Chloroflexus* is also similar to SQR complex of the aerobic, Gram-positive bacterium *B. subtilis* in terms of composition. The Cyt *b* polypeptide of *B. subtilis* SQR complex spans the cytoplasmic membrane with five α-helical transmembrane segments, and has the N-terminus in the cytoplasm. The same pattern of the second structure of *C. aurantiacus* mQFR can be obtained by hydropathy plot and sequence alignment (Supplemental data). These results show that the mQFR complex is a new member of the SQR/QFR superfamily. Some of these complexes such as *W. succinogenes* QFR and *B. subtili* SQR can generate a proton gradient through a redox loop mechanism in which electron transfer across the membrane is associated with the translocation of protons from the negative side to the positive side. A Q-cycle type mechanism [41], working inversely to that proposed for the cyt bc_1 complexes, had been proposed to explain the functional role of all prosthetic groups in these enzymes and add another energy conserving respiratory complex in these cells. However, some experimental results in *W. succinogenes* disproved the existence of an important site of quinone binding [42] and the relatedness of the oxidation of menaquinol to an electrogenic process [43]. A working hypothesis to reconcile the controversial results was proposed [44] based on the mutation work on *W. succinogenes* QFR [45], involving a key glutamate residue only conserved in mQFR and not in SQR. This hypothesis has since been supported by theoretical and experimental studies [9,46]. Whether the similar components might work in the thermophilic photosynthetic green bacterium *Chloroflexus* has not been investigated, considering the close relatedness in the phylogenetic analysis and possibly bi-functional mQFR found in both aerobic and anaerobic growth conditions.

In addition, *Chloroflexus* and its relatives contain a different pathway of autotrophic carbon fixation than is found in any other group of phototrophs, the 3-hydroxypropionate cycle [47,48]. In this cycle, acetyl CoA is carboxylated and reduced to form 3-hydroxypropionate, and a second carboxylation and reduction forms succinyl-CoA. Eventually, the two carbon acid glyoxylate is formed and serves as substrate for further carbon assimilation. The mQFR complex is involved in this pathway and the fumarate is not the terminal electron acceptor in the pathway. Thus, the function of the enzyme maybe more than just involved in the anaerobic respiration observed in other anaerobes such as *W. succinogenes*. Whatever the case, in vivo, the functionality of SQR/QFR may be controlled by the energetic state of the cell, but apparently turning a SQR into a QFR is not a simple event. It is predicted that the mechanism of the quinone redox loop is involved in control of respiration and photosynthesis in this early divergent bacterium [18]. Overall, it is clear that SQR/QFR are extremely versatile and diverse enzymes, and that even with four crystal structures available, many interesting problems remain to be tackled. Ongoing work includes establishing how the prosthetic groups of mQFR are tuned to work efficiently in the anaerobic photosynthetic cells and solving the crystal structure.

Acknowledgements

We thank Drs. Daniel Brune and John Lopez for their technical support for the MS measurement, Dr. Russ Lobrutto for EPR measurement, Dr. Meitian Wang for crystal screening and the staff of BL 8.2.1 in ALS and ID 19 in APS for X-ray diffraction measurements. This work was supported by grants to REB from the Exobiology Program from NASA and from the Molecular Biochemistry Program from NSF (Grant 0646621).

Appendix A. Supplementary data

Supplementary data associated with this article can be found, in the online version, at doi:10.1016/j.bbabio.2008.11.010.

References

[1] C. Hägerhäll, Succinate: quinone oxidoreductases. Variations on a conserved theme, Biochim. Biophys. Acta 1320 (1997) 107–141.
[2] T. Ohnishi, C.C. Moser, C.C. Page, P.L. Dutton, T. Yano, Simple redox-linked proton-transfer design: new insights from structures of quinol-fumarate reductase, Structure 8 (2000) R23–R32.
[3] C.R. Lancaster, Succinate:quinone oxidoreductase: an overview, Biochim. Biophys. Acta 1533 (2002) 1–7.
[4] C.R. Lancaster, A. Kröger, M. Auer, H. Michel, Structure of fumarate reductase from *Wolinella succinogenes* at 2.2 Å resolution, Nature 402 (1999) 377–385.
[5] T.M. Iverson, C. Luna-Chavez, G. Cecchini, D.C. Rees, Structure of the *Escherichia coli* fumarate reductase respiratory complex, Science 284 (1999) 1961–1966.
[6] V. Yankovskaya, R. Horsefiled, S. Tornroth, C. Luna-Chavez, H. Miyoshi, C. Leger, B. Byrne, G. Cecchini, S. Iwata, Architecture of succinate dehydrogenase and reactive oxygen species generation, Science 299 (2003) 700–704.
[7] F. Sun, X. Huo, Y. Zhai, A. Wang, J. Xu, D. Su, M. Bartlam, Z. Rao, Crystal structure of mitochondrial respiratory membrane protein complex II, Cell 121 (2005) 1043–1057.
[8] R.S. Lemos, A.S. Fernandes, M.M. Pereira, C.M. Gomes, M. Teixeira, Quinol: fumarate oxidoreductases and succinate:quinone oxidoreductases; phylogenetic relationships, metal centres and membrane attachment, Biochim. Biophys. Acta 1533 (2002) 158–170.
[9] M.G. Madej, H.R. Nasiri, N.S. Hilgendorff, H. Schwalbe, C.R.D. Lancaster, Evidence for transmembrane proton transfer in a dihaem-containing membrane protein complex, EMBO J. 25 (2006) 4963–4970.
[10] R.S. Lemos, C.M. Gomes, M. Teixeira, *Acidianus ambivalens* complex II typifies a novel family of succinate dehydrogenases, Biochem. Biophys. Res. Commun. 281 (2001) 141–150.
[11] A.S. Fernandes, M.M. Pereira, M. Teixeira, The succinate dehydrogenase from the thermohalophilic bacterium *Rhodothermus marinus*: redox-Bohr effect on heme bL, J. Bioenerg. Biomembr. 33 (2001) 343–352.
[12] R.S. Lemos, C.M. Gomes, J. LeGall, A.V. Xavier, M. Teixeira, The quinol:fumarate oxidoreductase from the sulphate reducing bacterium *Desulfovibrio gigas*: spectroscopic and redox studies, J. Bioenerg. Biomembr. 34 (2002) 21–30.
[13] T. Kurokawa, J. Sakamoto, Purification and characterization of succinate: menaquinone oxidoreductase from *Corynebacterium glutamicum*, Arch Microbiol. 183 (2005) 317–324.
[14] J.E. Butler, R.H. Glaven, A. Esteve-Núñez, C. Núñez, E.S. Shelobolina, D.R. Bond, D.R. Lovley, Genetic characterization of a single bifunctional enzyme for fumarate reduction and succinate oxidation in *Geobacter sulfurreducens* and engineering of fumarate reduction in *Geobacter metallireducens*, J. Bacteriol. 188 (2006) 450–455.
[15] M. Mileni, F. MacMillan, C. Tziatzios, K. Zwicker, A.H. Hass, W. Mäntele, J. Simon, C.R.D. Lancaster, Heterologous production in *Wolinella succinogenes* and characterization of the quinol:fumarate reductase enzymes from *Helicobacter pylori* and *Campylobacter jejuni*, Biochem J. 395 (2006) 191–201.
[16] B.K. Pierson, R.W. Cashtenholz, A phototrophic gliding filamentous bacterium of hot springs, *Chloroflexus aurantiacus*, gen. and sp. Nov, Arch. Microbiol. 100 (1974) 5–24.
[17] C.R. Woese, O. Kandler, M.L. Wheelis, Towards a natural system of organisms: proposal for the domains Archaea, Bacteria, and Eucarya, Proc. Natl. Acad. Sci. USA 87 (1990) 4576–4579.
[18] R.E. Blankenship, Molecular Mechanisms of Photosynthesis, Blackwell Science Inc., Oxford, UK, 2002.
[19] R.G. Feick, R.C. Fuller, Topography of the photosynthetic apparatus of *Chloroflexus aurantiacus*, Biochemistry 23 (1984) 3693–3700.
[20] M.B. Hale, R.E. Blankenship, R.C. Fuller, Menaquinone is the sole quinone in the facultatively aerobic green photosynthetic bacterium *Chloroflexus aurantiacus*, Biochim. Biophys. Acta 723 (1983) 376–382.
[21] R. Feick, J.A. Shiozawa, A. Ertlmaier, Biochemical and spectroscopic properties of the reaction center of the green filamentous bacterium, *Chloroflexus aurantiacus*, in: R.E. Blankenship, M.T. Madigan, C.E. Bauer (Eds.), Anoxygenic Photosynthetic Bacteria, Kluwer Academic Publisher, Dordrecht, The Netherlands, 1995, pp. 699–708.
[22] R.M. Wynn, T.E. Redlinger, J.M. Foster, R.E. Blankenship, R.C. Fuller, R.W. Shaw, D.B. Knaff, Electron transport chains of phototrophically and chemotrophically grown *Chloroflexus aurantiacus*, Biochim. Biophys. Acta 891 (1987) 216–226.
[23] M.F. Yanyushin, Fractionation of cytochromes of phototrophically grown *Chloroflexus aurantiacus*. Is there a cytochrome bc complex among them? FEBS Lett. 512 (2002) 125–128.
[24] M.F. Yanyushin, M.C. del Rosario, D.C. Brune, R.E. Blankenship, New class of bacterial membrane oxidoreductase, Biochemistry 44 (2005) 10037–10045.
[25] R.E. Blankenship, R. Feick, B.D. Bruce, C. Kirmaier, D. Holten, R.C. Fuller, Primary photochemistry in the facultative green photosynthetic bacterium *Chloroflexus aurantiacus*, J. Cell. Biochem. 22 (1983) 251–261.
[26] H. Schägger, G. von Jagow, Tricine-sodium dodecyl sulfate-polyacrylamide gel electrophoresis for the separation of proteins in the range of 1 to 100 kDa, Anal. Biochem. 166 (1987) 368–379.
[27] H. Schägger, G. von Jagow, Blue native electrophoresis for isolation of membrane protein complexes in enzymatically active form, Anal. Biochem. 199 (1991) 223–231.
[28] L. Hederstedt, Cytochrome b reducible by succinate in an isolated succinate dehydrogenase —cytochrome b complex from *Bacillus subtilis* membrane, J. Bacterial. 144 (1980) 933–940.

[29] P.E. Brumby, R.W. Miller, V. Massey, The content and possible catalytic significance of labile sulfide in some of metalloflavoproteins, J. Biol. Chem. 240 (1965) 2222–2228.
[30] J.E. Falk, Biochim. Biophys, Acta Library, Vol. 2, Elsevier Press, The Netherlands, 1964, p. 241.
[31] C. Hägerhäll, A. Roland, C. von Wachenfeldt, L. Hederstedt, Two hemes in *Bacillus subtilis* succinate: menaquinone oxidoreductase, Biochemistry 31 (1992) 7411–7421.
[32] W.J. Henzel, T.M. Billeci, J.T. Stults, S.C. Wong, C. Grimley, C. Watanabe, Identifying proteins from two-dimensional gels by molecular mass searching of peptide fragments in protein sequence databases, Proc. Natl. Acad. U. S. A. 90 (1993) 5011–5015.
[33] G.S. Wilson, Determination of oxidation–reduction potentials, Methods Enzymol. 54 (1978) 396–410.
[34] E. Lemma, C. Hägerhäll, V. Geisler, U. Brandt, G. von Jagow, A. Kröger, Reactivity of the *Bacillus subtilis* succinate dehydrogenase complex with quinones, Biochim. Biophy. Acta 1059 (1991) 281–285.
[35] A.H. Haas, C.R.D. Lancaster, Calculated coupling of transmembrane electron and proton transfer in dihemic quinol:fumarate reductase, Biophys. J. 87 (2004) 4298–4315.
[36] M.T. Werth, G. Cecchini, A. Manodori, B.A.C. Ackrell, I. Schröder, R.P. Gunsalus, M.K. Johnson, Site-directed mutagenesis of conserved cysteine residues in *Escherichia coli* fumarate reductase: modification of the spectroscopic and electrochemical properties if the [2Fe–2S] cluster, Proc. Natl. Acad. U. S. A. 87 (1990) 8965–8969.
[37] L. Hederstedt, Respiration without O_2, Science 284 (1999) 1941–1942.
[38] C.R.D. Lancaster, Succinate:quinine oxidoreductaseres—what can we learn from *Wolinella succinogenes* quinol:fumarate reductase? FEBS Lett. 504 (2001) 133–141.
[39] K.M. Robinson, B.D. Lemire, A requirement for matrix processing peptidase but not for mitochondrial chaperonin in the covalent attachment of FAD to the yeast succinate dehydrogenase flavoprotein, J. Biol. Chem. 271 (1996) 4061–4067.
[40] M.G. Bertero, R.A. Rothery, M. Palak, C. Hou, D. Lim, F. Blasco, J.H. Weiner, N.C. Strynadka, Insights into the respiratory electron transfer pathway from the structure of nitrate reductase A, Nat. Struct. Biol. 10 (2003) 681–687.
[41] M.M. Pereira, M. Teixeira, Is a Q-cycle-like mechanism operative in dihaemic succinate: quinone and quinol: fumarate oxidoreductases? FEBS Lett. 543 (2003) 1–4.
[42] J. Simon, R. Gross, M. Ringel, E. Schmidt, A. Kröger, Deletion and site-directed mutagenesis of the *Wolinella succinogenes* fumarate reductase operon, Eur. J. Biochem. 251 (1998) 418–426.
[43] M. Schnorpfeil, I.G. Janausch, S. Biel, A. Kroger, G. Unden, Generation of a proton potential by succinate dehydrogenase of *Bacillus subtilis* functioning as a fumarate reductase, Eur. J. Biochem. 268 (2001) 3069–3074.
[44] C.R.D. Lancaster, *Wolinella succinogenes* quinol: fumarate reductase — 2.2-Å resolution crystal structure and the E-pathway hypothesis of coupled trans-membrane proton and electron transfer, Biochim. Biophys. Acta 1565 (2002) 215–231.
[45] C.R.D. Lancaster, R. Gross, A. Haas, M. Ritter, W. Mäntele, J. Simon, A. Kröger, Essential role of Glu-C66 for menaquinol oxidation indicates transmembrane electrochemical potential generation by *Wolinella succinogenes*, Proc. Natl. Acad. U. S. A. 97 (2000) 13051–13056.
[46] M.G. Madej, H.R. Nasiri, N.S. Hilgendorff, H. Schwalbe, G. Unden, C.R.D. Lancaster, Experimental evidence for proton motive force-dependent catalysis by the diheme-containing succinate:menaquinone oxidoreductase from the Gram-positive bacterium Bacillus licheniformis, Biochemistry 45 (2006) 15049–15055.
[47] H. Holo, R. Sirevag, Autotrophic growth and CO_2 fixation of *Chloroflexus aurantiacus*, Arch. Mirobiol. 145 (1986) 173–180.
[48] S. Herter, G. Fuchs, A. Bacher, W. Eisenreich, A bicyclic autotrophic CO_2 fixation pathway in *Chloroflexus aurantiacus*, J. Biol. Chem. 277 (2002) 20277–20283.